0.3 km/s for events within 2 km; and 7.9 ± 0.1 km/s for events more than 2 km below the reflector. See table S1 for distribution.
21. B. R. Hacker, S. M. Peacock, G. A. Abers, *J. Geophys. Res.* **108**, 2030, 10.1029/2001JB001129 (2003).
22. J. F. Cassidy, R. M. Ellis, *J. Geophys. Res.* **98**, 4407 (1993).
23. For example, fault width = 2 × crustal thickness = 15 km for a fault plane subparallel to slab dip, twice as long as is wide = 30 km, having 1.5-m slip, rigidity of basalt = 5×10^{10} Pa gives, Mo = rigidity × width × length × slip = 3×10^{19} N-m, M_w = (2/3)log(Mo) − 6.06 = 7.0.
24. H. Dragert, K. Wang, T. S. James, *Science* **292**, 1525 (2001).
25. M. M. Miller, T. Melbourne, D. J. Johnson, W. Q. Sumner, *Science* **295**, 2423 (2002).
26. G. Rogers, H. Dragert, *Science* **300**, 1942 (2003).
27. K. Obara, *Science* **296**, 1679 (2002).
28. T. M. Brocher, T. Parsons, A. M. Trehu, C. M. Snelson, M. A. Fisher, *Geology* **31**, 267 (2003).
29. This study was supported by the U.S. Geological Survey and by the NSF. We thank the SHIPS Working Group (M. A. Fischer, T. Parsons, R. A. Hyndman, K. C. Miller, C. N. Snelson, D. C. Mosher, T. L. Pratt, R. Ramachandran, G. D. Spence, U. S. ten Brink, C. S. Weaver, and B. C. Zelt) for providing data and contributing to the success of the experiment, and for advice and discussions. We also thank N. P. Symmons for help with the tomography code; G. Medema, T. M. Van Wagoner, and Qing Xu for helpful discussions; and B. Hacker, R. Blakely, and P. McCrory for reviews.

Detection of a Human Influence on North American Climate

David J. Karoly,[1]* Karl Braganza,[2] Peter A. Stott,[3]
Julie M. Arblaster,[4] Gerald A. Meehl,[4]
Anthony J. Broccoli,[5]† Keith W. Dixon[5]

Several indices of large-scale patterns of surface temperature variation were used to investigate climate change in North America over the 20th century. The observed variability of these indices was simulated well by a number of climate models. Comparison of index trends in observations and model simulations shows that North American temperature changes from 1950 to 1999 were unlikely to be due to natural climate variation alone. Observed trends over this period are consistent with simulations that include anthropogenic forcing from increasing atmospheric greenhouse gases and sulfate aerosols. However, most of the observed warming from 1900 to 1949 was likely due to natural climate variation.

Most of the observed global-scale warming over the last 50 years is believed to have been due to the increase in atmospheric greenhouse gas concentrations (*1*). Here, we investigated the causes of climate change in the North American region over the 20th century with the use of a number of simple indices of large-scale surface temperature variation. These indices represent different aspects of both natural climate variability and the expected climate response to increasing greenhouse gases (*2*). Previous studies of the possible causes of 20th-century climate change have concentrated on global-scale patterns of temperature change (*3*). The magnitude of any greenhouse gas–induced climate change signal relative to natural climate variability decreases as the spatial scale of consideration is reduced (*4*). This explains the focus of most climate change detection and attribution studies on global scales. Recently, it has been shown that an anthropogenic climate change signal may be detectable in the North American region by analysis of surface temperature changes over the past 50 years (*5, 6*).

Significant changes in North American temperatures occurred during the second half of the 20th century (*1, 7*). We investigated the causes of these changes by comparing observed temperature changes during the 20th century to simulations performed with five different climate models. The simulations represent the natural internal variability of climate as well as its response to human influences, such as increases in atmospheric greenhouse gases and sulfate aerosols. Natural external influences (changes in solar irradiance and volcanic aerosols) are also included. We sought to identify whether there has been a significant human influence on observed surface temperature changes in the North American region over the 20th century.

We used a small number of indices of area-average surface temperature variation (*2*). These were chosen to represent different aspects of climate variation in the North American region, defined here as a rectangular region (30° to 65°N, 40° to 165°W) encompassing the United States and Canada and the surrounding ocean region. The simple indices are as follows: NA, North American area-mean surface air temperature over land; LO, mean land-ocean temperature contrast (area-mean temperature over land minus the mean sea surface temperature for the surrounding region); MTG, meridional temperature gradient in the North American region [mean temperature over land in higher latitudes (Canada, 50° to 70°N) minus that in middle latitudes (United States, 30° to 50°N)]; AC, mean magnitude of the annual cycle in temperature over land [area-mean temperature in summer (June–August) minus that in winter (December–February)]; and DTR, mean diurnal temperature range over land (area-mean daily maximum temperature minus minimum temperature).

The indices represent the main features of the modeled surface temperature response to increasing greenhouse gases, such as faster warming over land than over ocean, faster warming in winter than in summer, faster warming of nighttime minima than of daytime maxima, and faster warming at higher latitudes. Because the indices (apart from NA) are defined as differences, they are likely to contain information independent of that in NA. In addition, defining indices on the basis of large area averages significantly enhances the signal-to-noise ratio, increasing the likelihood of climate change detection (*5*).

Observed seasonal-mean gridded surface temperature data for the period 1881 to 1999 (*8*) were used to calculate the indices. These data were obtained from quality-controlled instrumental observations and have been used in virtually all detection studies considering surface temperature changes. Observed diurnal temperature range data were obtained from a different data set (*9*). Annual means were constructed using seasonal averages from December of the previous year to November. Because high-latitude areas have fewer data available for the early part of the 20th century, we stipulated that only regions with data available throughout most of the 20th century were considered in the analysis. This yields a time-invariant data "mask," which was applied to both the observations and climate model output before the calculation of the indices. The time series of annual means were low-pass filtered (*10*) to estimate variability on decadal time scales.

[1]School of Meteorology, University of Oklahoma, Norman, OK 73019, USA. [2]School of Mathematical Sciences, Monash University, Clayton, Victoria 3800, Australia. [3]Hadley Centre, MetOffice, Bracknell RG12 2SY, UK. [4]National Center for Atmospheric Research (NCAR), Boulder, CO 80307, USA. [5]Geophysical Fluid Dynamics Laboratory, National Oceanic and Atmospheric Administration, Princeton, NJ 08542, USA.

*To whom correspondence should be addressed. E-mail: dkaroly@ou.edu
†Present address: Department of Environmental Sciences, Rutgers University, New Brunswick, NJ 08901, USA.

The observed temperature changes over the 20th century were compared to simulations with five global coupled ocean-atmosphere climate models (*11*): GFDL R30 (Geophysical Fluid Dynamics Laboratory, USA); HadCM2 and HadCM3 (Hadley Centre, UK); ECHAM4 (Max-Planck-Institut für Meteorologie, Germany); and PCM (National Center for Atmospheric Research, USA). All the climate models include representations of important physical processes in the atmosphere and the ocean, as well as sea-ice and land-surface processes. Three of the models (GFDL R30, HadCM2, and ECHAM4) include adjustments of heat and freshwater fluxes at the surface to reduce climate drift in the coupled model simulations. The other two models (HadCM3 and PCM) have no flux adjustments and maintain stable global-mean climates when external forcings are not varied.

Such constant external forcing simulations ("control runs") represent the natural internal variability of the unforced climate system (*12*). We also analyzed simulations that represent the human influence on climate, including changing concentrations of atmospheric greenhouse gases, ozone, and sulfate aerosols (GS runs) (*13*), and simulations that represent the climate response to natural external forcings, including changing solar irradiance and volcanic aerosol amounts in the stratosphere (NAT runs) (*14*).

The observed variability of the detrended indices on interannual and decadal time scales was compared with the variability in control climate model simulations to evaluate the quality of the simulations of natural internal climate variability. Simple linear detrending was used to attempt to remove any possible anthropogenic signal in the observed indices. The results are insensitive to the order of the polynomial trend removed from the indices. There is very good agreement between the decadal variability of the model simulations and the observed variability for all the indices, apart from the variability of the MTG (Fig. 1). The variability of the MTG is significantly higher than observed for all the models except HadCM3. Although a recent review (*15*) has noted that simulations with climate models generally overestimate the variability of temperatures over the continents, this does not seem to be the case for the models and most of the indices considered here.

Next, we compared the observed linear trends in the indices over the first and second halves of the 20th century, as well as the whole century, with anthropogenically forced (GS) model simulations (Fig. 2). The uncertainty in the forced model response was reduced by using the ensemble-mean response for each model (*13, 14*). The variability of 50-year and 100-year trends due to internal climate variability was estimated from the long control runs (*16*).

Over the period 1900 to 1949, the increase in observed NA is significantly different from zero (Fig. 2A). The observed warming trend is outside the 90% confidence interval (centered on zero) for natural internal variability (*16*). For the other indices, the observed trends are close to zero. This indicates that the land and surrounding oceans warmed at

similar rates over this period, and that the United States and Canada warmed at similar rates. The ensemble-mean North American warming from the GS model simulations is much smaller than the observed warming trend during 1900–1949. However, if the uncertainty due to natural internal variability is combined with the uncertainty for the en-

Fig. 1. Standard deviations of decadal variations of the different indices from the control model simulations and observations. The observational data had a simple linear trend removed before calculating the standard deviation. The error bars on the model values are the approximate 90% confidence intervals for the standard deviation, estimated by resampling the long control model simulations (*16*). No error bars are shown for the ECHAM4 model because only 240 years of control run output was available.
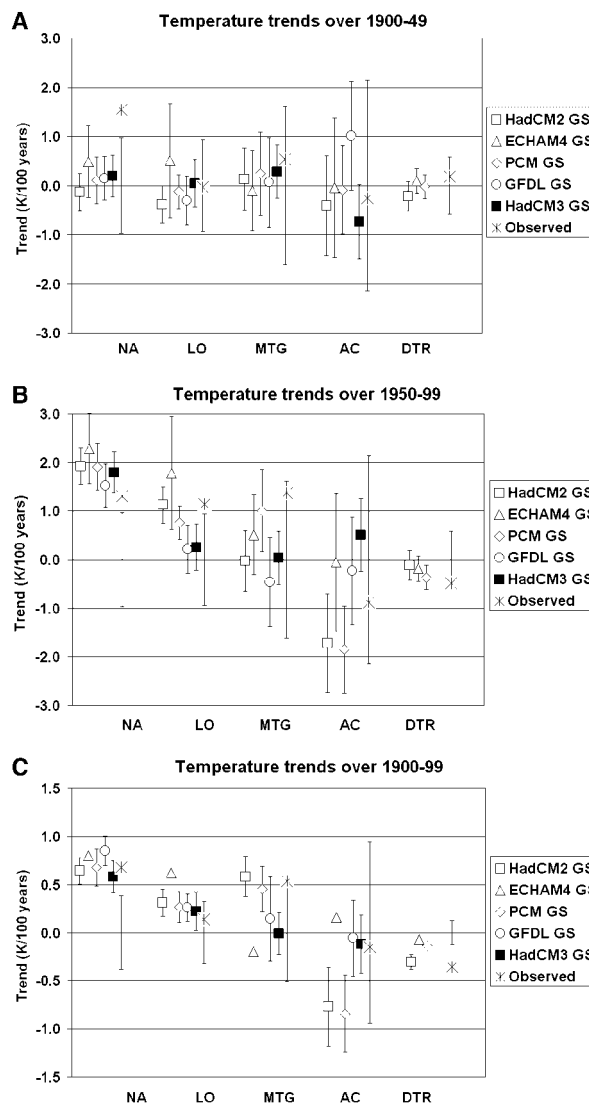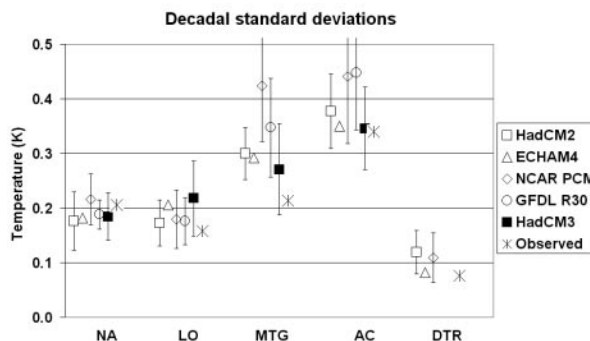
Fig. 2. Trends in the anthropogenically forced (GS) model simulations and in the observations over (**A**) 1900–1949, (**B**) 1950–1999, and (**C**) 1900–1999. The error bars on the model trends are the 90% confidence intervals for the ensemble-mean trends, estimated by resampling the long control simulations from the respective models and allowing for the number of members in each ensemble (*16*). The error bars about zero at the location of the observed trends are the uncertainties in the trend estimates due to natural internal climate variability, as simulated by the models. They are the 90% confidence intervals for a single realization, estimated using the control simulations from the ECHAM4, HadCM2, and PCM models, which were the only ones with DTR data available (*16*).

semble-mean response, there is a small chance that the observed warming could be explained as weak anthropogenic warming combined with a case of unusually large multidecadal warming due to natural internal variations (about 5% chance for the GFDL, HadCM3, and PCM models; much smaller chance for the HadCM2 model; much greater chance for the ECHAM4 model because of the greater uncertainty of its GS ensemble mean and greater simulated warming).

Over the period 1950 to 1999, the increases in observed NA and LO are significantly different from zero (Fig. 2B). The observations also show an increase in MTG and reductions in DTR and AC, but these are not significant. The observed trends in all the indices during 1950–1999 are consistent with the response to anthropogenic forcing in the GS models (17).

Over the period 1900 to 1999, the increases in observed NA and MTG and decrease in observed DTR are significantly different

from zero (Fig. 2C). The observed increase in LO and decrease in AC are not significant. Again, the observed trends in all the indices are consistent with the response to anthropogenic forcing in the models, except for DTR, where the observed decrease is larger than the trends in all the model simulations and is significantly larger than in the PCM and ECHAM4 model simulations. This disagreement between the observed trend and the model simulations for DTR has several possible interpretations, including neglect of other possibly important forcings, errors in the forcings that were included, or problems with the model responses to the applied forcings.

A number of studies have indicated a possible contribution from changes in natural external forcings (solar irradiance and volcanic aerosols) to the observed global warming in the first half of the 20th century (3, 18, 19). In the following, we use four climate models to investigate whether natural external forcing can explain the observed trends in NA

(Fig. 3); output from naturally forced simulations was not available from the ECHAM4 model. For both 1950–1999 and 1900–1999, the observed warming trend over North America is very similar to each model's response to anthropogenic forcing and is significantly larger than the model responses to natural forcing alone (Fig. 3). For 1900–1949, the response to natural forcing in all four models is consistent with the observed warming and larger than the response to anthropogenic forcing.

Time series of low-pass filtered ensemble-mean North American average temperatures from the GS model simulations are in good agreement with the observed warming in the second half of the 20th century but do not show the observed warming in the first half of the century (Fig. 4). The NAT model simulations do not show warming in the second half of the century and are clearly separated from the observations and GS simulations in the later part of the century. There is remarkable agreement between the response to natural forcing in the GFDL model in the first half of the century and the observed warming. However, the volcanic forcing used in combination with this GFDL model may have caused an overestimation of the volcanic response, contributing to the model warming over 1900–1949 in response to the decrease in volcanic aerosol forcing (20).

Significant changes can be seen in several of the indices over the second half of the 20th century and over the whole century, including NA, LO, MTG, and DTR. It is likely that the observed increases in NA over 1950–1999 and 1900–1999 cannot be explained by natural climate variations alone. The observed trends over the second half of the century for all the indices are consistent with the response to anthropogenic (GS) forcing in these models. It is likely that anthropogenic climate change made only a small contribution to the observed warming over 1900–1949 and that changes in natural external forcing, solar irradiance, and volcanic activity were significant influences on the North American warming during this period. Climate model simulations with combined changes in anthropogenic and natural forcings are likely to better capture the observed trends over the 20th century.

We have confidence in the results because they are very similar for all the models, despite differences in the model formulations and differences in the representations of the anthropogenic and natural forcings. However, we have not considered some other possible anthropogenic forcings, such as changes in land cover or the role of carbon black and other nonsulfate aerosols, which are likely to be somewhat more important on regional than on global scales.

Fig. 3. Trends in North American mean temperature from anthropogenically forced (GS, open symbols) and natural externally forced (NAT, solid symbols) model simulations and observations during 1900–1949, 1950–1999, and 1900–1999. The error bars on the model trends are the 90% confidence interval for the ensemble-mean trend, estimated by resampling the respective long control model simulations and allowing for the number of members in each ensemble

North American mean temperature trends

(16). The error bars about zero at the location of the observed trends are the uncertainties in the trend estimates due to natural internal climate variability, as simulated by the models. They are the 90% confidence intervals for a single realization, estimated using the control simulations from the ECHAM4, HadCM2, and PCM models (16).
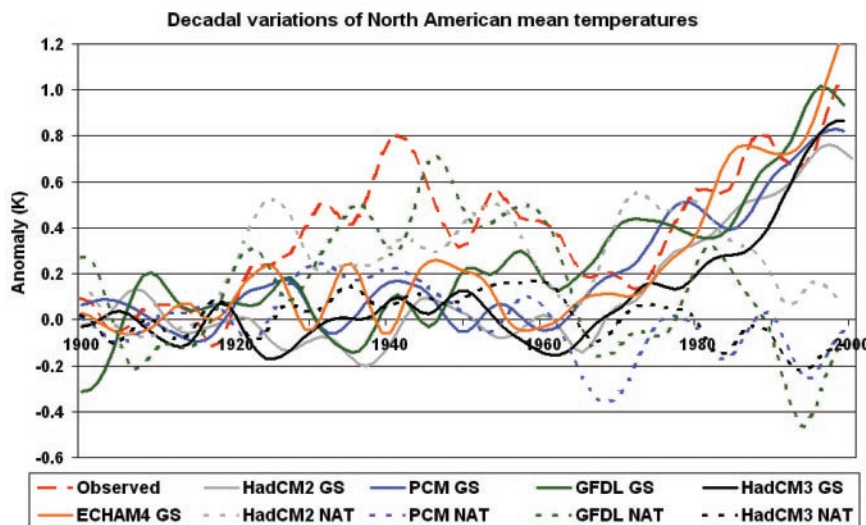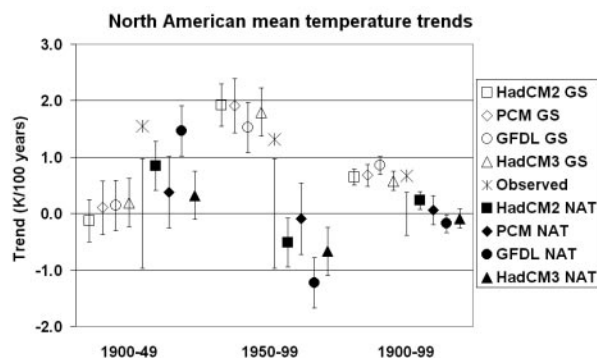
Fig. 4. Time series of low-pass filtered North American mean temperature anomalies from observations (long-dashed red line) and ensemble-mean model simulations with variations in anthropogenic forcing (GS, solid lines) or natural external forcing (NAT, short-dashed lines). NAT simulations were available only for the HadCM2, GFDL, PCM, and HadCM3 models.

On the basis of these results, it is likely that there has been a significant human influence on the observed North American warming in the second half of the 20th century, associated with increasing atmospheric concentrations of greenhouse gases and sulfate aerosols. Over the 20th century, this influence is manifest not only in mean temperature changes but also in changes of the north-south temperature gradient, the temperature contrast between land and ocean, and reduction of the diurnal temperature range.

References and Notes

1. J. T. Houghton *et al.*, Eds., *Climate Change 2001: The Scientific Basis* (Cambridge Univ. Press, Cambridge, 2001).
2. K. Braganza *et al.*, *Clim. Dyn.* **20**, 491 (2003).
3. J. F. B. Mitchell *et al.*, in *Climate Change 2001: The Scientific Basis*, J. T. Houghton *et al.*, Eds. (Cambridge Univ. Press, Cambridge, 2001), pp. 695–738.
4. P. A. Stott, S. F. B. Tett, *J. Clim.* **11**, 3282 (1998).
5. F. W. Zwiers, X. Zhang, *J. Clim.* **16**, 793 (2003).
6. P. A. Stott, *Geophys. Res. Lett.* **30**, 1728 (2003).
7. T. R. Karl, R. W. Knight, D. R. Easterling, R. G. Quayle, *Bull. Am. Meteorol. Soc.* **77**, 279 (1996).
8. P. D. Jones, M. New, D. E. Parker, S. Martin, I. G. Rigor, *Rev. Geophys.* **37**, 173 (1999).
9. M. New, M. Hulme, P. D. Jones, *J. Clim.* **13**, 2217 (2000), updated by T. Mitchell at the Climatic Research Unit, University of East Anglia.
10. We applied a low-pass, 21-point binomial filter (half power at periods near 10 years), as used in the Intergovernmental Panel on Climate Change (IPCC) assessment (*1*).
11. A brief description of the five climate models is provided in the Supporting Online Material, together with references to publications providing more details.
12. For each of the models, we used data from long control simulations that have been performed with no changes to the external forcing parameters. The control simulations include 990 years of data from HadCM2, 1830 years from HadCM3, 500 years from GFDL R30, 240 years from ECHAM4, and 530 years from NCAR PCM. The 530-year period from PCM came from years 390 to 919 of the control run, after most of the initial climate drift had stabilized. Data for DTR were not available from the HadCM3 model and could not be determined from the GFDL model, which does not include a diurnal cycle of solar irradiance.
13. The anthropogenically forced model simulations include anthropogenic changes in well-mixed greenhouse gases, ozone (for some of the models), and sulfate aerosols. The major changes in radiative forcing are due to the changes in greenhouse gases and sulfate aerosols, so these are described as GS simulations. For the GFDL and HadCM2 models, these changes are expressed as an increase in equivalent CO_2 according to IPCC scenario IS92a for the period 1880–2000, along with estimated observed changes in anthropogenic sulfate aerosols represented through regional changes to surface albedo. For the HadCM3 (*21*), ECHAM4, and PCM (*22*) models, observed increases in individual major anthropogenic greenhouse gases are included, together with changes in tropospheric and stratospheric ozone and an explicit treatment of the direct radiative effect of sulfate aerosols. HadCM3 and ECHAM4 also include parameterizations for indirect sulfate forcing effects via cloud albedo changes. From HadCM2 and HadCM3, we have four independent members of an ensemble of simulations with different initial conditions, three GS ensemble members from GFDL R30, two from ECHAM4, and seven from PCM.
14. The natural externally forced model simulations include fixed greenhouse gas concentrations and estimated changes in total solar irradiance and stratospheric volcanic aerosol optical depth for the period 1880–1999. Somewhat different solar and volcanic forcing data sets are used for the different models. For the HadCM2 (three ensemble members) and HadCM3 (four ensemble members) simulations, the solar forcing is based on Lean *et al.* (*23*) and the volcanic forcing is based on updated data from Sato (*24*). For the GFDL model (*20*), the solar forcing is based on Lean (*25*) and the volcanic forcing is based on Andronova *et al.* (*26*). For the NCAR PCM simulations (*27*) (four ensemble members), the solar forcing is based on Hoyt and Schatten (*28*) and the volcanic forcing is based on Ammann *et al.* (*29*). For the GFDL model, simulations with natural external forcing alone were not available, so the NAT response was estimated from the difference between model simulations with all forcings (both anthropogenic forcing and natural external forcing, three ensemble members each) and simulations with anthropogenic forcing alone (three ensemble members); that is, NAT response ~ (GS + NAT) response – GS response. For the HadCM2 model, only simulations with separate solar (SOL) and volcanic (VOL) forcing were available, so the NAT response was estimated as the sum of these model responses; that is, NAT response ~ SOL response + VOL response.
15. J. Bell, P. B. Duffy, C. Covey, L. Sloan, *Geophys. Res. Lett.* **27**, 261 (2001).
16. The uncertainty of the ensemble mean 50-year and 100-year trends due to natural internal variability was estimated by resampling trends from the long control simulations from the respective models and allowing for the number of members in each ensemble. Further details of the approach used for estimating natural internal variability are given in the Supporting Online Material.
17. Consistency here means that the observed trend lies within the 90% confidence interval for the ensemble-mean forced trend (shown as the error bar about the forced model trend) combined with the 90% confidence interval for a single realization due to natural internal climate variability (shown as the error bar about zero trend).
18. S. F. B. Tett, P. A. Stott, M. R. Allen, W. J. Ingram, J. F. B. Mitchell, *Nature* **399**, 569 (1999).
19. P. A. Stott, S. F. B. Tett, M. R. Allen, J. F. B. Mitchell, G. J. Jenkins, *Science* **290**, 2133 (2000).
20. A. J. Broccoli *et al.*, in preparation.
21. T. C. Johns *et al.*, *Clim. Dyn.* **20**, 583 (2003).
22. B. D. Santer *et al.*, *Science* **301**, 479 (2003).
23. J. Lean, J. Beer, R. Bradley, *Geophys. Res. Lett.* **22**, 3195 (1995).
24. M. Sato, J. E. Hansen, M. P. McCormick, J. Pollack, *J. Geophys. Res.* **98**, 22987 (1993).
25. J. Lean, *Geophys. Res. Lett.* **27**, 2425 (2000).
26. N. G. Andronova, E. V. Rozanov, F. Yang, M. E. Schlesinger, G. L. Stenchikov, *J. Geophys. Res.* **104**, 16807 (1999).
27. G. A. Meehl, W. M. Washington, T. M. L. Wigley, J. M. Arblaster, A. Dai, *J. Clim.* **16**, 426 (2003).
28. D. V. Hoyt, K. H. Schatten, *J. Geophys. Res.* **98**, 18895 (1993).
29. C. Ammann, G. A. Meehl, W. M. Washington, C. Zender, *Geophys. Res. Lett.* **30**, 1657 (2003).
30. We acknowledge the assistance of the many scientists who developed the observational data sets and the climate models used in this study. Constructive comments from a number of reviewers helped to improve this manuscript. Supported by a Discovery grant from the Australian Research Council (K.B.); the UK Department for Environment, Food and Rural Affairs under contract PECD 7/12/37 (P.A.S.); and NSF and the Office of Biological and Environmental Research, U.S. Department of Energy (J.M.A., G.A.M.).

Ice Core Evidence for Antarctic Sea Ice Decline Since the 1950s

Mark A. J. Curran,[1]* Tas D. van Ommen,[1] Vin I. Morgan,[1] Katrina L. Phillips,[2] Anne S. Palmer[2]

The instrumental record of Antarctic sea ice in recent decades does not reveal a clear signature of warming despite observational evidence from coastal Antarctica. Here we report a significant correlation ($P < 0.002$) between methanesulphonic acid (MSA) concentrations from a Law Dome ice core and 22 years of satellite-derived sea ice extent (SIE) for the 80°E to 140°E sector. Applying this instrumental calibration to longer term MSA data (1841 to 1995 A.D.) suggests that there has been a 20% decline in SIE since about 1950. The decline is not uniform, showing large cyclical variations, with periods of about 11 years, that confuse trend detection over the relatively short satellite era.

Evidence from observations covering the past ~40 years indicates that parts of coastal Antarctica are warming (*1*, *2*), yet there has been a lack of supporting evidence (*2–5*) from a key warming indicator (*6*), namely sea ice. This is primarily due to high regional variability in sea ice coverage (*3*) and the absence of long-term observations. Antarctic sea ice plays a vital role in climate control, ocean-atmosphere heat exchange, ocean circulation, and ecosystem support (*7–10*). Understanding these important roles of sea ice requires an awareness of the variability in sea ice extent (SIE) and the time scales of change.

Little information is available on sea ice trends beyond the last couple of decades, raising several questions: How useful are recent trends in assessing long-term variability? Is Antarctic sea ice in decline? If so, is this decline an effect of global warming? The advent of regular passive microwave information in 1973 has allowed

---

[1]Department of the Environment and Heritage, Australian Antarctic Division, and Antarctic Climate and Ecosystem Cooperative Research Centre, Private Bag 80, Hobart, Tasmania 7001, Australia. [2]Institute of Antarctic and Southern Ocean Studies, University of Tasmania, Private Bag 77, Hobart, Tasmania 7001, Australia.

To whom correspondence should be addressed. E-mail: mark.curran@utas.edu.au